UCLA
COMPUTATIONAL AND APPLIED MATHEMATICS

Numerical Investigation of 2D Laminar Flow and Solute Transport in a Channel with Some Symmetric Expansion and Contractions

O. P. Iliev

July 1993

CAM Report 93-30

Department of Mathematics
University of California, Los Angeles
Los Angeles, CA. 90024-1555

NUMERICAL INVESTIGATION OF 2D LAMINAR FLOW AND SOLUTE TRANSPORT IN A CHANNEL WITH SOME SYMMETRIC EXPANSIONS AND CONTRACTIONS

O.P. Iliev *

Abstract

Numerical investigation of 2D laminar flow and solute transport in a channel with some sudden symmetric expansions and contractions have been performed using fictitious regions method. This method allows us instead of solving Navier-Stokes equations in a complex domain, to solve equations with suitably continued coefficients in a rectangle. Stream function-vorticity variables are used in the present paper. Dependence of the flow and solute transport from the dimensions of the channel expansions and contractions is numerically investigated for different values of Reynolds and Peclet numbers using a finite differences method.

1. Introduction

Flow and solute transport in a channel with some symmetric expansions and contractions have to be studied in many cases as a part of different physical and technological problems - say, in bioreactors, chemical reactors, etc. However, the complexity of the considered domain sometimes restricts the possibilities for numerical investigations of the current there processes.

In the present paper the flow and the solute transport in a complex domain are numerically studied (see Figure 1). The 2D Navier-Stokes equations in stream function - vorticity variables are employed to describe the laminar flow of incompressible viscous fluid and a convection-diffusion conservation of mass equation is employed to describe the solute transport. Fictitious regions method is used to overcome the non-uniformity of the considered domain. An upwind, linearized finite difference scheme on an uniform grid approximates the system of PDE's mentioned above. First of all, a steady-state velocity field is computed and after that convection-diffusion equation is solved for determining solute transport in the region. The parametric analysis of the considered problem is performed.

The remainder of the paper is organized as follows. In the next section a mathematical model is described. Section 3 is devoted to a numerical algorithm explanation. Results from numerical experiments are presented in Section 4.

2. Mathematical Model

We consider a half of a 2D plane channel with some symmetric expansions and contractions, as shown in Figure 1, and note it by G. The symmetric expansions and contractions form cavities and each cavity is followed by step. We will denote by G_{f_l} the left-corner step, by G_{f_r} - the right-corner step and by G_{f_i} the interior steps. All existed steps form a G_f

*Institute of Mathematics, Bulgarian Academy Sciences, Acad.G.Bonchev str.,bl.8,1113 Sofia, Bulgaria.

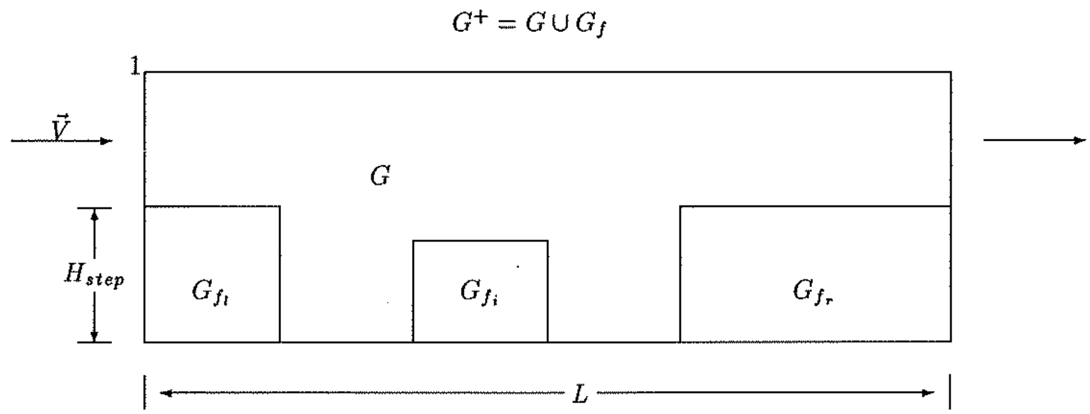

FIGURE 1

domain. Supposing that the flowing liquid is a viscous incompressible one, and introducing stream function ψ and vorticity ω by equalities

$$u = \frac{\partial \psi}{\partial y}, \qquad v = -\frac{\partial \psi}{\partial x}, \qquad \omega = \frac{\partial v}{\partial x} - \frac{\partial u}{\partial y},$$

the following equations (see, for example [1,2]) in Cartesian co-ordinates (x,y) can be used:

$$u\frac{\partial \omega}{\partial x} + v\frac{\partial \omega}{\partial y} = \frac{1}{Re}\Delta\omega, \tag{1}$$

$$\Delta\psi = -\omega, \qquad (x,y) \in G. \tag{2}$$

The bottom boundary of G is supposed to be no-slip and impermeable. At the inflow boundary Poisseule flow is considered. The symmetry conditions are employed at the centerline. Soft boundary conditions are used at the outflow boundary. So, we have (see,for example, [2])

$$\psi = 1, \qquad \frac{\partial \psi}{\partial n} = 0 \qquad \textit{at the bottom boundary} \tag{3a}$$

$$\psi = \frac{3}{2H}\left(Y - \frac{Y^3}{3H^2}\right), \qquad \omega = \frac{3Y}{H^3}, \qquad \textit{at the inflow boundary for } x = 0, \tag{3b}$$

$$\psi = \omega = 0 \qquad \textit{at the centerline for } y = 0, \tag{3c}$$

$$\frac{\partial \psi}{\partial x} = \frac{\partial \omega}{\partial x} = 0 \qquad \textit{at the outflow boundary for } x = L. \tag{3d}$$

Here $H = 1 - H_{step}$, $Y = 1 - y$ and n stand for outer normal.

The unsteady convection-diffusion transport of solutable component is governed by the following conservation of mass equation:

$$\frac{\partial C}{\partial t} + u\frac{\partial C}{\partial x} + v\frac{\partial C}{\partial y} = \frac{1}{Pe_D}\Delta C, \qquad (x,y) \in G. \tag{4}$$

The top and bottom boundaries are supposed to be impermeable for the solute. On the inlet boundary a Dirichlet boundary condition is considered. The soft boundary condition is used on the outlet boundary. So, we have:

$$\begin{cases} C(0,y) = 1 & \text{at the inlet boundary,} \\ \frac{\partial C}{\partial n} = 0, & \text{on the other boundaries.} \end{cases} \tag{5}$$

The variables and the function in the dimensionless equations above are scaled with respect to the inlet average velocity $\vec{V}$, doubled height of the left-corner step H_{step}, and some value of the diffusivity coefficient D. Re, and Pe_D stand for Reynolds and diffusivity Peclet numbers, respectively. Note, that only forced convection is considered, and dependence of the concentration gradient on the velocity field is neglected. Designations are described in the nomenclature.

3. Numerical Algorithm

We will compute the steady-state solution of Equations (1)–(3) as a time limit of the solution of the unsteady equations. Let G^+ denotes the rectangle $(0,L)\times(0,1)$. So, G^+ is the union of the domain G of the channel with some sudden symmetric expansions and constructions, with the left-corner step G_{f_l}, with the right-corner step G_{f_r}, and with the inside steps G_{f_i}. All this steps form the fictitious region, which is denoted by G_f To overcome the difficulties with solving Navier-Stokes equations in the complex domain G, we will use the fictitious regions method. This method was suggested by Saul'yev in 1960 for solving elliptical problems [3]. The essence of the method is described in the monograph [4] and the mostly complete description of the fictitious regions method and its applications to hydrodynamics problems can be find in the monograph [5].The main idea of this method is to solve the equations with suitably extended coefficients in the rectangle G^+, instead of solving Equations (1)–(3) in the complex domain G. We will use a variant of the fictitious regions method for fourth order equations (see, for example, [5]). So, instead of Equations (1) and (2), let us consider the fourth-order equation for the stream function:

$$u\frac{\partial \Delta\psi}{\partial x} + v\frac{\partial \Delta\psi}{\partial y} = \frac{1}{Re}\Delta\Delta\psi \qquad (x,y)\in G. \tag{6}$$

In this case the use of the fictitious regions method is reduced to the following procedure: instead of problem (6) in the domain G, we solve a problem which gives us the approximate solution in the rectangle G^+. This approximation to ψ (denoted by ψ_ϵ) is a solution of the equation

$$u_\epsilon\frac{\partial \Delta\psi_\epsilon}{\partial x} + v_\epsilon\frac{\partial \Delta\psi_\epsilon}{\partial y} = \frac{1}{Re}\Delta\Delta\psi_\epsilon + c_\epsilon\cdot\psi_\epsilon. \qquad (x,y)\in G^+ \tag{7}$$

with the corresponding boundary conditions on ∂G^+. The concentration field can be determined by the equation

$$\frac{\partial C_\epsilon}{\partial t} + u_\epsilon\frac{\partial C_\epsilon}{\partial x} + v_\epsilon\frac{\partial C_\epsilon}{\partial y} = \frac{1}{Pe_D}\Delta C_\epsilon - c_\epsilon\cdot C_\epsilon. \qquad (x,y)\in G^+ \tag{8}$$

The extended coefficient c_ϵ in (7) and (8) is defined as follows:

$$c_\epsilon = \begin{cases} 0, & (x,y)\in G, \\ \epsilon^{-2}, & (x,y)\in G^+\backslash G. \end{cases}$$

To find a numerical solution of the system of PDE's above we use the finite difference method [6]. We introduce in G^+ an uniform rectangular grid with steps h_x and h_y respectively. The difference scheme used here is based on the results of papers [7,8]. Let us first write the equation (7) in a differential-difference form.

$$\frac{\partial \Lambda\psi}{\partial t} + A_c\Lambda\psi = \frac{1}{Re}\Lambda\Lambda\psi - c_\epsilon \cdot \psi \tag{9}$$

Note, that in the above equation and below the grid-functions are denoted by the same letters, as continue ones, and subscript ϵ is omitted everywhere. By Λ is denoted a grid operator, approximating 2D Laplace operator on the uniform grid.By A_c is denoted a grid operator, approximating convective terms. Let us now replace $\Lambda\psi$ in (9) by

$$\Lambda\psi = -\omega$$

So, we have

$$\frac{\partial \omega}{\partial t} + A_c\omega = \frac{1}{Re}\Lambda\omega - c_\epsilon \cdot \psi \tag{10}$$

The following additive approximation difference scheme is used for time-approximation of equation (10):

$$\frac{\bar{\omega} - \omega}{\tau} + A_c\bar{\omega} = \frac{1}{Re}\Lambda\bar{\omega} - c_\epsilon \cdot \psi \tag{11}$$

$$\frac{\hat{\omega} - \bar{\omega}}{\tau} + c_\epsilon \cdot \left(\hat{\psi} - \psi\right) = 0 \tag{12}$$

Here $\hat{\omega}$ stands for the value of the vorticity on the new time level $\hat{\omega} = \omega\left(x_i, y_j, t^{k+1}\right)$ and $\bar{\omega}$ stands for vorticity value on some middle time level.

An implicit, hybrid central differences – upwind differencing scheme, which has second-order approximation in the subregions of small gradients of the solution, is used in the present paper for approximation of convective terms:

$$A_c\bar{\omega} = \frac{u^+_{i-1,j}}{2}\bar{\omega}_{\bar{x}\ i,j} - \frac{u^-_{i+1,j}}{2}\bar{\omega}_{\bar{x}\ i+1,j} - \frac{v^-_{i,j+1}}{2}\bar{\omega}_{\bar{y}\ i,j+1} + \frac{v^+_{i,j-1}}{2}\bar{\omega}_{\bar{y}\ i,j}$$
$$+\frac{u^+_{i+1,j}}{2}\omega_{\bar{x}\ i+1,j} - \frac{u^-_{i-1,j}}{2}\omega_{\bar{x}\ i,j} - \frac{v^-_{i,j-1}}{2}\omega_{\bar{y}\ i,j} + \frac{v^+_{i,j+1}}{2}\omega_{\bar{y}\ i,j+1}$$

where

$$\omega_{\bar{x}i,j} = \frac{\omega_{i,j} - \omega_{i-1,j}}{h_x}, \qquad u^+_{i,j} = \frac{u_{i,j} + \mid u_{i,j} \mid}{2}, \qquad etc.$$

Now we replace ω in (12) with

$$\hat{\omega} = -\Lambda\hat{\psi} \tag{13}$$

and obtain an equation for computation stream function on the new time level:

$$\Lambda\hat{\psi} - \tau c_\epsilon\hat{\psi} = -\bar{\omega} - \tau c_\epsilon\psi \tag{14}$$

The order of calculations is as follows. First, the vorticity is determined from the equation (11) and corresponding boundary conditions. Based on our previous experience [9], the iterative method of an approximate factorization-conjugate gradients in version [10] is used for solving a nonsymmetric set of linear algebraic equations. Next, the stream function is computed from (14) using the symmetric variant of the iterative method mentioned above. The last, velocity components are computed and vorticity is corrected using equation (13), and then the procedure is repeated successfully to reach a steady-state solution of the Navier-Stokes equations. After steady-state velocity components are computed, the linear unsteady convection/diffusion transport equation for the concentration is solved in the similar way.

4. Results from the Numerical Experiments

Numerical algorithm validation. To check validity of the numerical algorithm described above, some numerical experiments with flow in a channel with a sudden symmetric expansion have been done and results are compared with the results from other papers. The stream function maximum values and the values of a reattachment length, computed by the present algorithm, and available from [11] and [12], are presented in Table 1. It is shown, that there exist a good agreement between presented data. A small differences can be caused by the different approximations of the convective terms, used in different papers. In Fig.2 streamlines are presented for a repeat flow in a channel with a sudden symmetric expansion for $Re = 50$. Here and below the following values are used plotting streamlines: 0.1, 0.3, 0.5, 0.7, 0.9, 1.0, 1.01, 1.02, 1.04, 1.06.

Table 1.

Re	ψ_{max}	ψ_{max}-present	reattachment length	reattachment length-present
46.6	1.044 [11]	1.0370	3.17 [11]	3.15
50	1.0412 [12]	1.0402		3.64
100	1.0476 [12]	1.0470		6.02

Different cavities' lengths. In Fig.3 the streamlines for for flow in a channel with three equidimensional cavities are shown for different cavities' dimensions. The used grid has 201×81 nodes, $Re = 100$, cavities' height is $h = 0.5$ and the distance between cavities is $d = 0.5$. It is shown, that the eddies are practically the same in each of the repeated cavities on each of the three pictures, presented on Fig.3. The stream function maximum values in each of the cavities, for these and other experiments, are given in Table 2. The similarity of the flow in the repeated cavities for the considered symmetric problem (1)–(3) can be observed independently of the distance between cavities, as it can be seen on some of the next pictures. As one can expect, the eddy is stronger for longer cavities, as it is observed in Fig.3. The concentration field for two of of the flows, shown in Fig.3, are presented in Fig.4 for $Pe = 10$. The concentration field, in general, is different in each of the repeated cavities. So, it is important to have a possibility to compute the real concentration field for real bio- and chemical reactors, which in many cases include the system of repeated cavities.

Different Re numbers. The streamlines for flow in a channel with three equidimensional cavities is presented in Fig.5 for $Re = 10$, $Re = 100$ and $Re = 400$. The used grid has 201×81 nodes, $h = 0.5, l = 2.0, d = 0.25$. The stream function maximum values are given in Table 2. Let us note that the eddies in the repeated cavities are practically the same, as it was mentioned discussing Fig.3.

Different Pe numbers. The concentration field for $Pe = 10$ and $Pe = 100$ are shown in Fig.6. They are computed for the flow, presented in Fig.5, bottom picture, that is for $Re = 400$. It is shown in Fig.6, that if the diffusivity is stronger(that is, the diffusivity Peclet number is less), then the concentration fields in the repeated cavities are different. On the other hand, for larger Peclet number the concentration field in each of the repeated cavities tends to be the same. But, of course, the quantity of the solute in a cavity is less for larger Peclet number, due to dominating of convective mass transport over the diffusive mass transport in this case.

Different heights of an inside step. At the end, some results from numerical experiments for flow and solute transport in a channel with an inside step, in the case of different heights of the corner steps and the inside step, are presented. In Fig.7 the streamlines and the concentration field are shown for the case of inside step height $h = 0.25$. The used grid has 121×81 nodes, $Re = 100$. In Fig.8 the streamlines and the concentration field for $h = 0.75$ are presented.

Table 2.

Re	h	l	d	ψ_{max} in 1st cavity	ψ_{max} in 2nd cavity	ψ_{max} in 3rd cavity
100	0.5	2.0	0.5	1.045	1.044	1.050
100	0.5	2.0	0.25	1.046	1.044	1.048
100	0.5	2.0	0.0	1.045	1.045	1.058
100	0.5	1.0	0.5	1.044	1.044	1.045
10	0.5	2.0	0.25	1.013	1.015	1.015
400	0.5	2.0	0.25	1.057	1.055	1.056
100	0.25	1.0	1.0	1.043	1.017	
100	0.75	1.0	1.0	1.070	1.221	

Conclusions

Presented results confirm the necessity of computation of solute transport for full system of repeated cavities, instead of considering processes in all the cavities as fully identical. The fictitious regions method allows such computations to be performed with reasonable accuracy for reasonable run time.

Aknowlegments

This work is supported in part by Bulgarian Department of Science and Education under Grant MM–78/91 and from NSF under Grant INT-92-20287.

Nomenclature

u, v	–	velocity components
x, y	–	Cartesian coordinates
L	–	domain length
$\vec{V}$	–	average inlet velocity
ν	–	viscosity
D	–	mass diffusivity
C	–	composition
ψ	–	stream function
ω	–	vorticity
ϵ	–	fictitious regions method parameter
H_p	–	the left-corner step height
h	–	inside step height
l	–	cavity length
d	–	distance between cavities (steps width)
h_x, h_y	–	uniform grid steps

Reynolds Number: $$Re = \frac{V \cdot H_{step}}{\nu}$$

Diffusivity Peclet Number: $$Pe_D = \frac{V \cdot H_{step}}{D}$$

References

1. L.D. Landau and E.M.Lifshitz, *Fluid Mechanics*, 2nd Edition, Pergamon Press, 1987.

2. P.J. Roache, *Computational Fluid Dynamics*, Hermosa Publisher, 1972.

3. V.K. Saul'ev, On a method for computer solution of boundary values problems, *Doklady Academii Nauk SSSR*, **144**,497-500(1962). (in Russian).

4. G.I. Marchuk, *Methods of Computational Mathematics*, Moscow, Nauka, 1980 (in Russian).

5. P.N. Vabishchevich, *Fictitious Regions Method in Mathematical Physics Problems*, Moscow University Publishing House, 1991 (in Russian).

6. A.A. Samarskii, *Theory of Difference Schemes*, Nauka, Moscow, (1983).(in Russian)

7. P.N. Vabishchevich, Implicit difference schemes for nonstationary Navier-Stokes equations in variables of the flow-vortex function, *Diff. Equations* **20**(1984), 820–827.

8. P.N. Vabishchevich, Numerical realization of the fictitious regions methods for nonstationary Navier-Stokes equations, *Chisl. Methody Sploshnoy Sredy* **16**(1985), Novosibirsk, 19–27 (Russian).

9. O.P. Iliev, M.M. Makarov, and P.S. Vassilevski, Performance of certain iterative methods in solving 2D unsteady Navier-Stokes equations, *Int. J. Num. Meth. Engng.*, **33**(1992), 1465.

10. M.M. Makarov and A.B. Koutcherov, Some variants of alternating-triangular method for approximate factorizations of finite difference elliptic equations, *Numerical Methods for the Solution of Mathematical Physics Problems*, Moscow State University, Moscow, Viniti Publ., 1986, 130–173.

11. R.K. Agarwal, A third-order-accurate upwind scheme for Navier - Stokes solutions at high Reynolds numbers, *AIAA pap.*, 81-0112.

12. G.C.Georgiou, W.W. Schultz, and L.G. Olson, Singular finite elements for sudden symmetric expansion and for die–swell problem, *Int. J. Num. Meth. Fluids*, **10**,No.4, 357–372(1990)

Fig. 2.

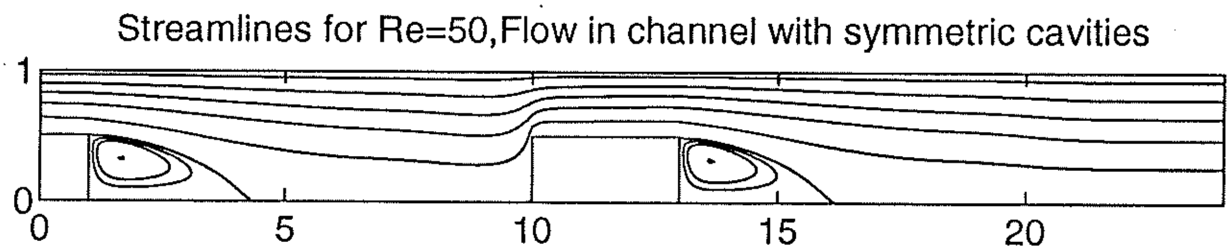

Streamlines for Re=50,Flow in channel with symmetric cavities
1
0
0
5
10
15
20

Fig. 3.

Flow in channel with symmetric cavities,Re=100,h=0.5,d=0.5

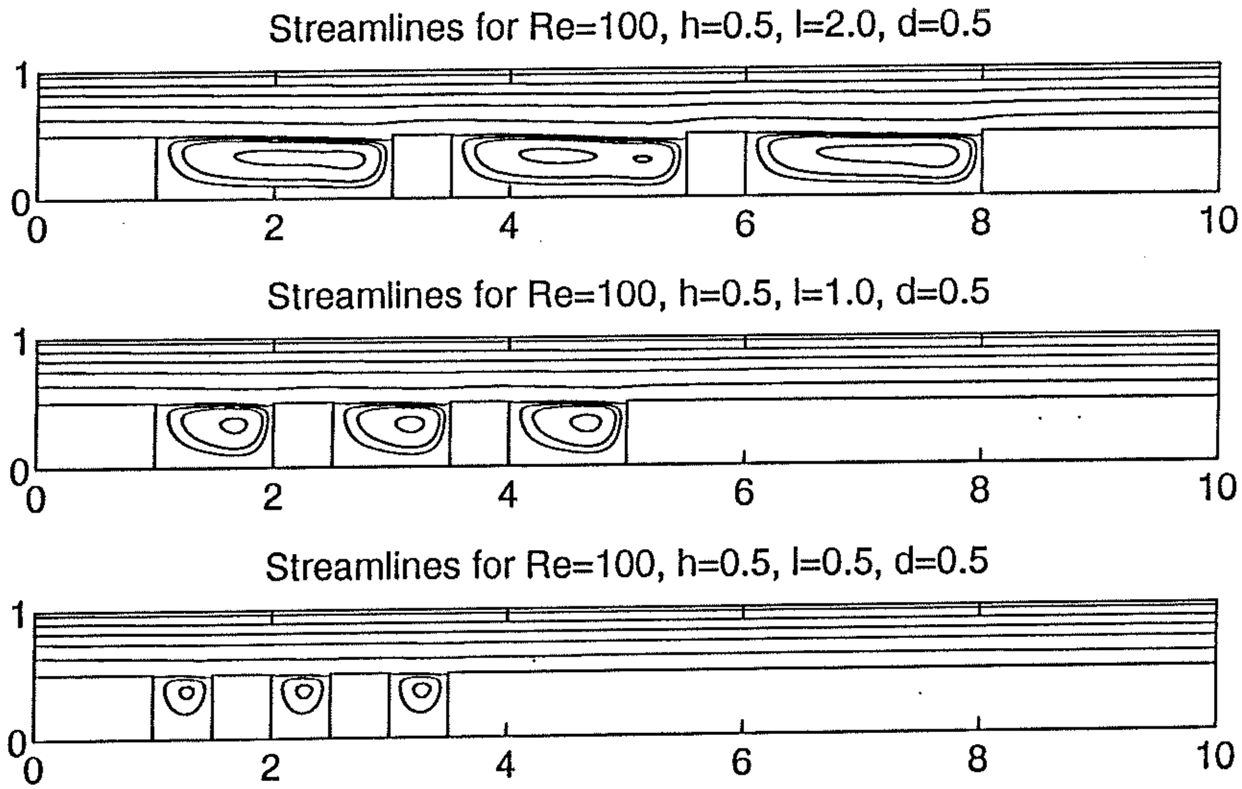

Fig. 4.

Concentration.(Flow in channel with symmetric cavities,Re=100)

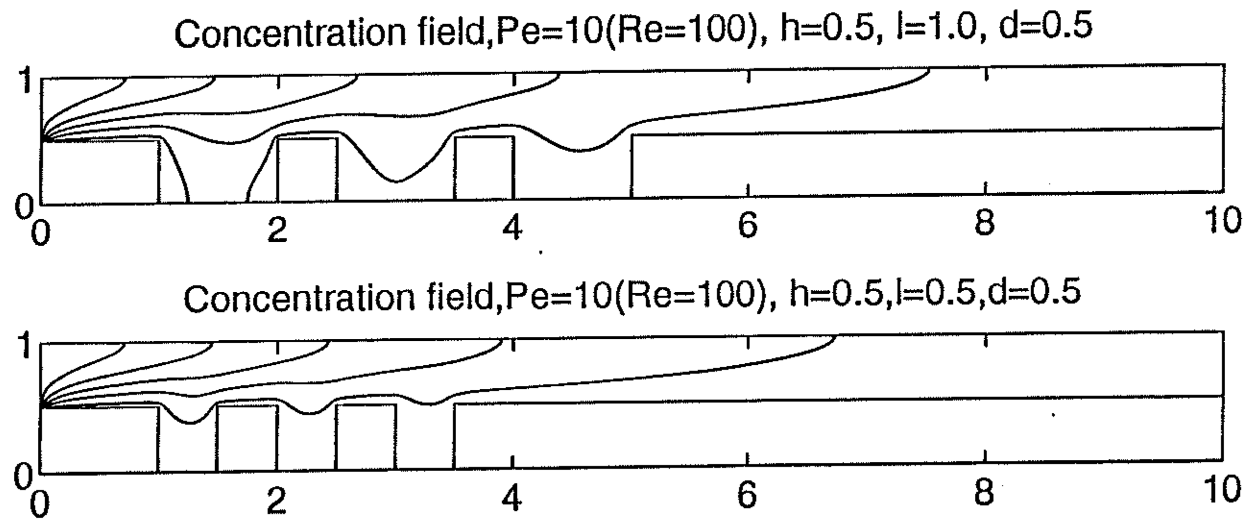

Fig. 5.

Flow in channel with symmetric cavities

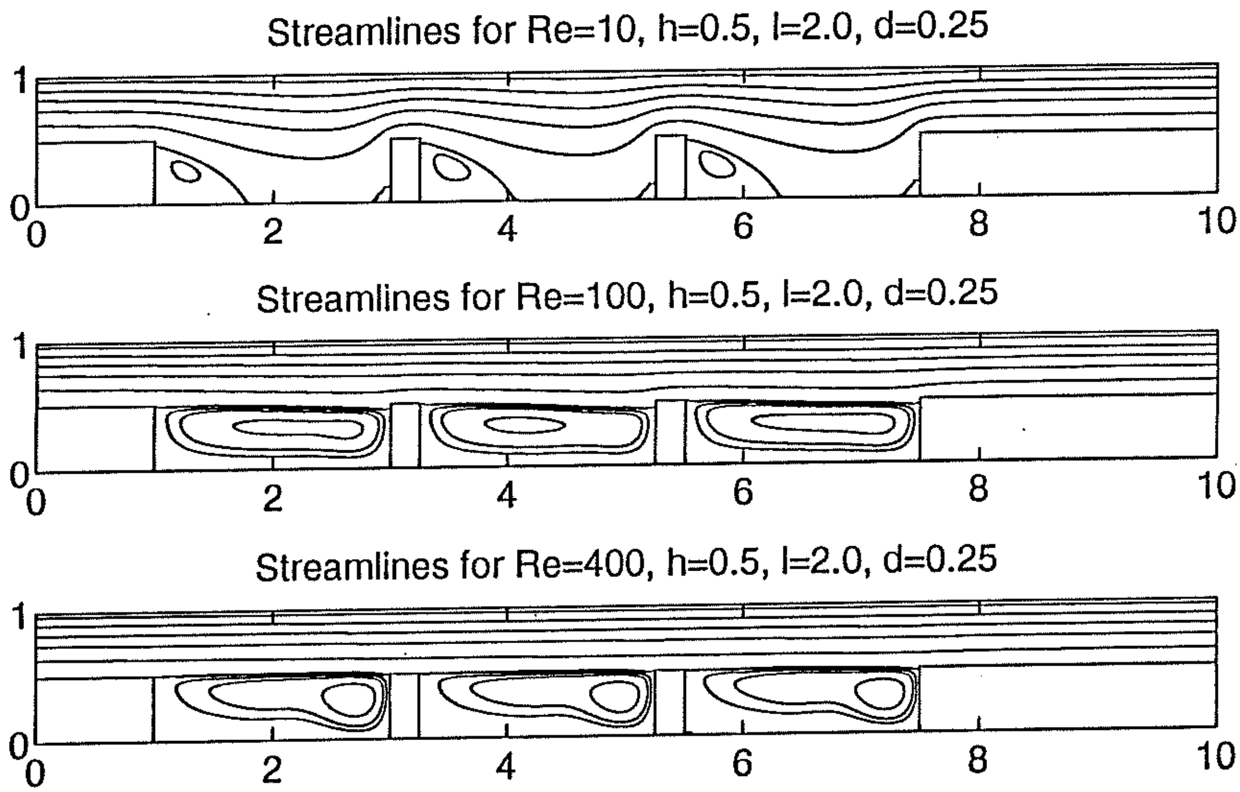

Fig. 6.

Concentration.(Flow in channel with symmetric cavities,Re=400)

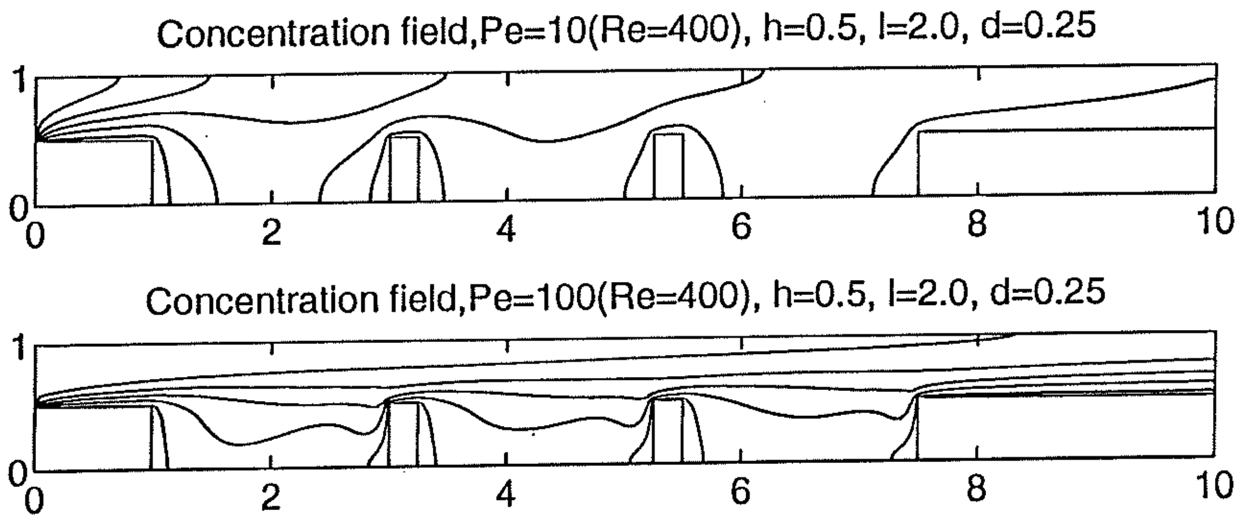

Fig. 7.

Flow in channel with symmetric cavities,Re=100

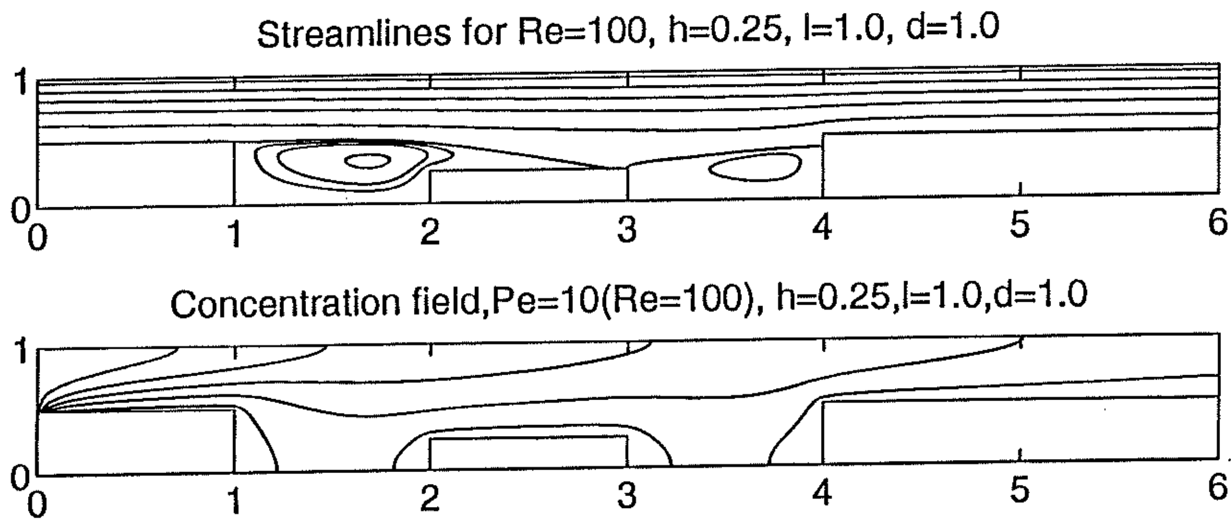

Fig. 8.

Flow in channel with symmetric cavities,Re=100